Design of a multi-spectral channel for in-vivo confocal microscopy

Houssine Makhlouf, Anthony A. Tanbakuchi, Andrew R. Rouse, Arthur F. Gmitro
College of Optical Sciences and the Department of Radiology
University of Arizona, PO Box 245067, Tucson, AZ 85724

ABSTRACT

We present a modified multi-spectral configuration of a slit-scanning confocal microendoscope that provides higher spectral resolution in a fully automated interface. Tissue fluorescence signal is directed through a dispersive element that spreads the spectral information across the CCD camera mapping spectral information perpendicular to the confocal slit. The dispersive element may be chosen to meet the specific requirements defined by the user. Our current system uses a BK7 prism with a 45° wedge angle and a 20mm diameter clear aperture. The prism is shifted from the optical axis allowing automated switching from grayscale (beam on-axis) to multi-spectral (beam off-axis) imaging by tilting a computer controlled mirror. The system records over a spectral range of 450nm to 750nm. The minimum resolvable wavelength difference varies from 2.1nm to 8.3nm over the spectral range. The lateral and axial resolution of the system is approximately 3µm by 30µm, respectively, and is the same for both grayscale and multi-spectral imaging modes. Multi-spectral imaging results from ex-vivo tissues are presented.

Keywords: microscopy, confocal, spectral, dispersion, prism

1 INTRODUCTION

In-vivo confocal microendoscopy can provide cellular-level images that have the potential to help pathologists make a diagnosis in-situ without the need to employ traditional tissue extraction biopsy methods. Such an optical biopsy instrument is beneficial in that it constitutes a minimally invasive procedure that provides instant visualization of pathology. We have developed a grayscale imaging system that has shown significant promise as a diagnostic instrument and is currently being tested in an in-vivo human clinical trial to investigate its use for diagnosis of ovarian cancer.

While most confocal microendoscopy systems record the entire fluorescence intensity signal in a single grayscale image, we have developed a multi-spectral imaging mode that provides additional in-vivo diagnostic information by measuring the fluorescence signal as a function of wavelength. The multi-spectral confocal microendoscope has the potential to provide improved diagnostic information. For example, quantitative measurements, such as nuclear to cytoplasmic ratio, could be obtained using organelle-specific fluorophores with unique spectral properties. Knowledge of this ratio could be very useful for pathologists who often look for enlarged nuclei as one of the morphologic indicators of cancer.

In this paper, we present a brief review of the grayscale imaging capabilities of our system and then give a full description of the newly designed multi-spectral system. Details of the grayscale mode of operation, along with the general concepts for a multi-spectral mode of operation, are described in previous publications[1-10].

2 SYSTEM DESIGN

2.1 Grayscale mode of operation

Figure 1 shows the layout of our confocal microendoscope under grayscale operation. A 488nm solid-state laser from Coherent[11] is used as the excitation source, with an Oz Optics[12] fiber coupler. After going through an anamorphic optical system, a line of illumination is formed and coupled into the proximal end of the catheter by an Olympus 10X microscope objective. A single axis scan mirror is used to scan the line of illumination across the face of the catheter. Figure 1 also shows the orthogonal view of the system from the orientation that has optical power in the cylindrical lens. A 30,000 element Sumitomo Electric[13] coherent imaging fiber bundle transmits the illumination line to the distal end of the catheter. The illumination profile is then imaged into the tissue by a miniature objective lens attached to an automated focus mechanism that enables depth selection down to 200µm below the tissue surface. Fluorescence light from the sample is collected back into the system via the fiber bundle and separated from the reflected illumination by a dichroic beam splitter. The fluorescence signal is then focused onto the confocal slit aperture, which rejects the collected light from out-of-focus planes. A second scan mirror and imaging optics direct the light passing through the confocal slit onto a Photometrics[14] Cascade II CCD camera.

A 2D grayscale image is acquired by synchronously scanning the two mirrors such that the illumination profile scans across the tissue while the image is scanned across the CCD. The grayscale system operates at 30 frames per second with a lateral and axial resolution of approximately 3µm and 30µm, respectively. The system is relatively compact (1' by 2' without the camera), and has relatively few optical components providing excellent throughput and stability. The system is fully automated with respect to the scan mirrors, laser power, and focus mechanism.
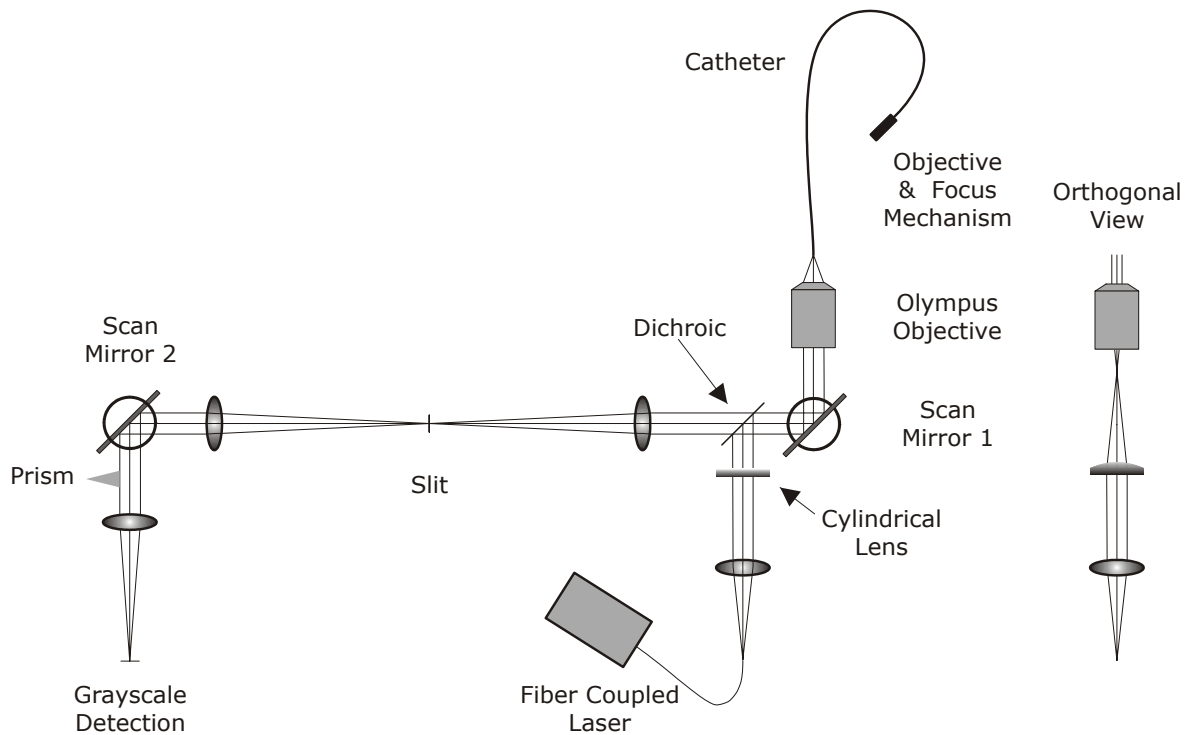

Figure 1 Layout of the clinical prototype confocal microendoscope in grayscale imaging mode. The orthogonal view shows the illumination path from the cylindrical lens power direction.

2.2 Multi-spectral mode of operation

In an early proof of principle demonstration of multi-spectral confocal microendoscope imaging, a fixed mirror was inserted in the beam path after the confocal slit aperture to divert the light through a dispersive prism onto a second CCD camera. For the new system, we wanted to build a multi-spectral imaging channel that required no additional components beyond the dispersing element. In addition, we wanted the ability to rapidly switch between multi-spectral

and grayscale imaging modes. We also wanted to have a large spectral bandwidth (450nm to 750nm) with sufficient spectral resolution to resolve features of common fluorescent dyes.

To address these constraints a design was developed whereby the prism is inserted outside the grayscale optical path and the second scan mirror is used to direct the light into the prism as shown in Figure 2. With this design the same camera is used for grayscale and multi-spectral imaging and selection of multi-spectral imaging mode is achieved simply by moving the second scan mirror to a fixed angle. The prism is used at its minimum deviation angle to simplify the system alignment and calibration. The prism was chosen to meet the optical requirements in terms of deviation and dispersion. It is a right angle prism with a 45° wedge angle and 20mm clear aperture made of BK7 glass. It is located 22mm away from the optical axis and is used with a camera lens that has a 180mm focal length and 60mm diameter entrance pupil.
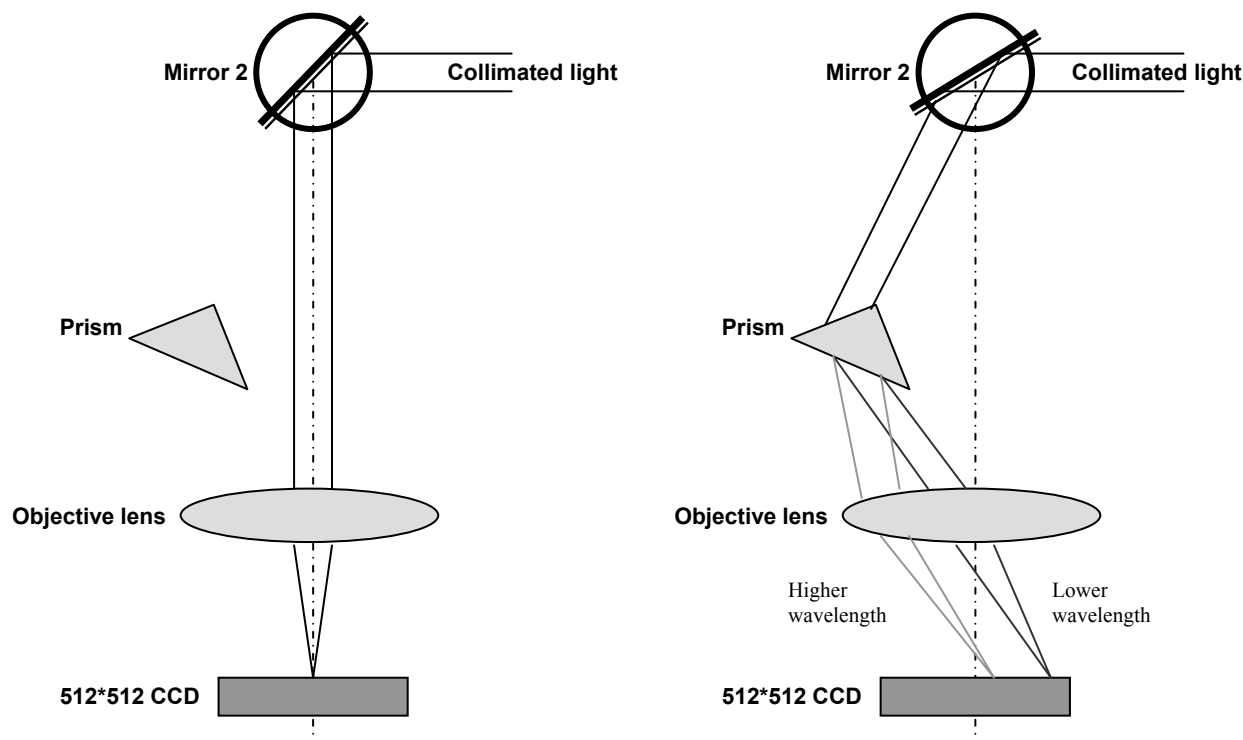

Figure 2 *(Left)* Grayscale and *(Right)* multi-spectral beam paths. Shorter wavelengths exit the prism with the largest deviation angle. Dispersed light is focused on a CCD camera located at the focal plane of the camera lens. The position on the detector is directly related to wavelength. Mirror 2 is stationary in multi-spectral mode.

The process of mirror control and data collection has been automated. To switch from grayscale to multi-spectral imaging mode the computer controlled galvo mirror (Scan Mirror 2) is rotated to a fixed position. The fluorescence signal, reflected by this mirror, is then dispersed by the prism and focused on the CCD camera at different locations according to wavelength. For each position of first scan mirror (Scan mirror 1), the system records the light signal pattern on the CCD, which has one spatial dimension (along the slit direction) and one spectral dimension (perpendicular to the slit direction). Performing this process (reading out a frame of data from the 2D detector) for every position of the first scan mirror allows us to reconstruct a 3D data cube that consists of two spatial dimensions and one spectral dimension. A calibration procedure employing a theoretical dispersion profile is used to map the measured spectrum as a function of wavelength (rather than detector pixel location). We discuss the details of the calibration technique in the following section.

3 DISPLAY PROGRAM

3.1 Representation of the multi-spectral data

We have developed an intuitive interface to display and evaluate the multi-spectral datasets collected by our system. Figure 3 shows the application interface (the image shown represents the light transmitted through the catheter and emitted by a lamp filtered to a 10nm bandwidth centered at 700nm). The acquired 3D data cube is represented as an unfolded cube that lays over a 2D surface. The main window shows the 2D spatial distribution of the sample at a selected wavelength, whereas the side views show the distributions of single vertical and horizontal lines of spatial information as a function of wavelength. The interface is interactive: a mouse click anywhere on the 2D image will plot the spectrum associated with that point and update the side views to show the spectral information along the horizontal and vertical lines through the selected point. A mouse click on a wavelength value in the side views will update the spatial 2D image to this wavelength.
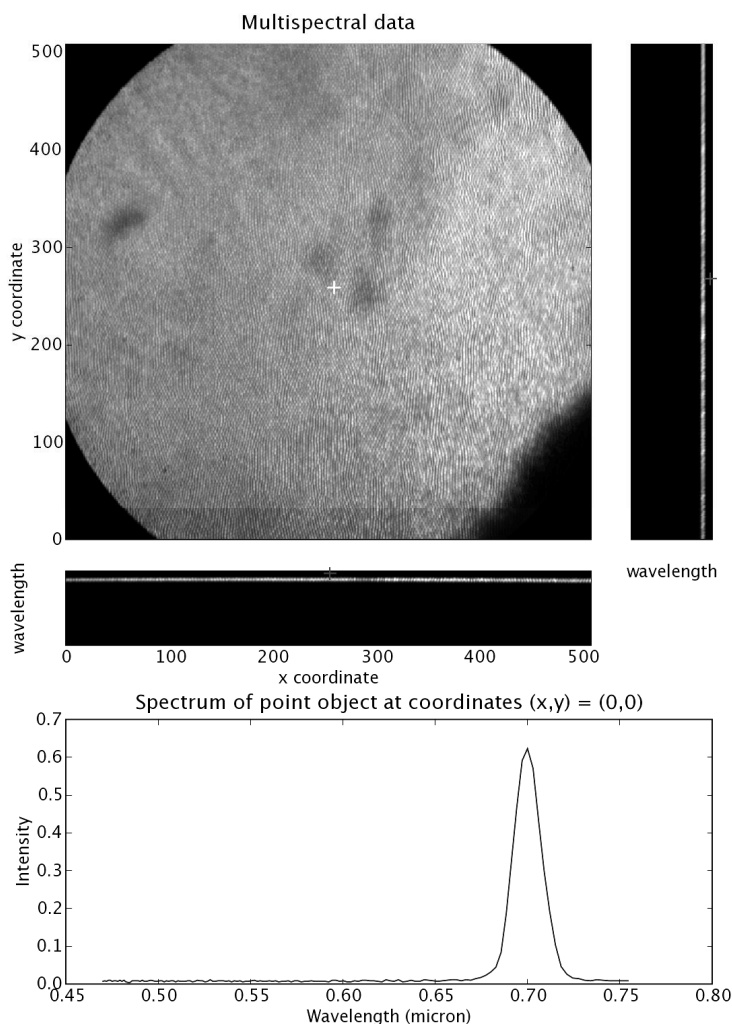

Figure 3 Light coming from a lamp after passing a 700nm optical filter (10nm band pass). *(Top)* Unfolded data cube and *(Bottom)* spectrum of the image point indicated by the white cross. A relative scale is used for the intensity.

Figure 4 shows the displayed image of a mark made with a pink highlighter at two different wavelengths (two cross-sectional image planes at two different wavelengths). We can see that the image does not show the same intensity when observed at a different wavelength.
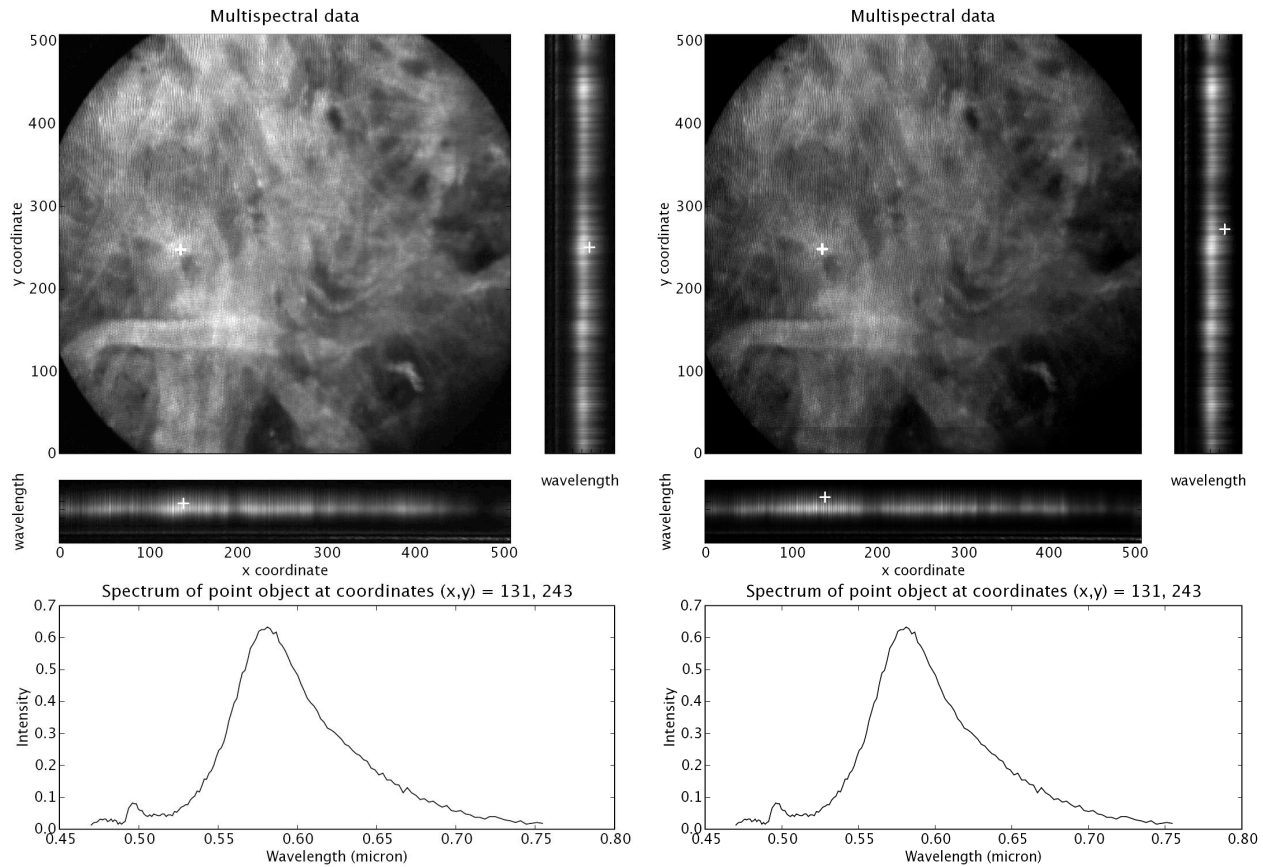
Figure 4 Image of paper marked with a pink highlighter. The right figure shows the fluorescent image at a longer wavelength than the left figure, which displays the 2D spatial information at the peak fluorescence wavelength. These data show decreased image intensity when looking at a spectral plane located away from the fluorescence peak. The spectrum is the same on both pictures since it comes from the same image point.

3.2 Multi-spectral calibration and wavelength scaling

A computer algorithm, based on the prism characteristics (BK7 glass, 45° wedge angle) and the focal length of the camera lens (180mm), is used to determine how the different wavelengths deviated by the prism in the range 450nm to 750nm map to an arbitrary detector in terms of pixel position. A single narrow-band wavelength measurement is then sufficient to calculate the shift necessary to adjust this theoretical profile to our specific system. In other words, by simply recording the signal coming from a lamp filtered by a 10nm band pass filter centered at a known wavelength we are able to associate each of the CCD camera pixels with wavelength.

4 PERFORMANCE AND RESULTS

4.1 Performance

The multi-spectral mode of the confocal microendoscope provides the same spatial resolution as that of the grayscale mode of operation, that is to say 3μm lateral and 30μm axial resolution. A 3D dataset consisting of 150 spectral samples is collected in about 8 seconds. The spectral resolution is defined as the minimum resolvable wavelength difference. It corresponds to the detection of two spectral peaks separated by 2 camera pixels (Rayleigh criteria), which is 32μm for our detector. Because refractive index is a function of wavelength, the dispersion of light through the prism is not constant, and therefore neither is the spectral resolution. Our system achieves a spectral resolution of 2.1nm at a wavelength of 450nm and 8.2nm at 750nm.

4.2 Results

Our initial experiment was performed on a microscope slide consisting of 15μm diameter microspheres with different fluorescent emission spectra. Figure 5 shows an image of these microspheres at two different wavelengths, corresponding to two different cross-section planes of the multi-spectral data cube. We can easily notice that some beads are visible at the high wavelength (639nm), but not at the low wavelength (578nm). Figure 6 shows the spectra associated with two different locations on the image of the microspheres. From the spectral information we can see that two groups of microspheres are present in the sample. The first group has a peak of emission around 0.64μm (Figure 6 - Top right), while the second group has a peak of emission at 0.60μm (Figure 6 – Bottom right).
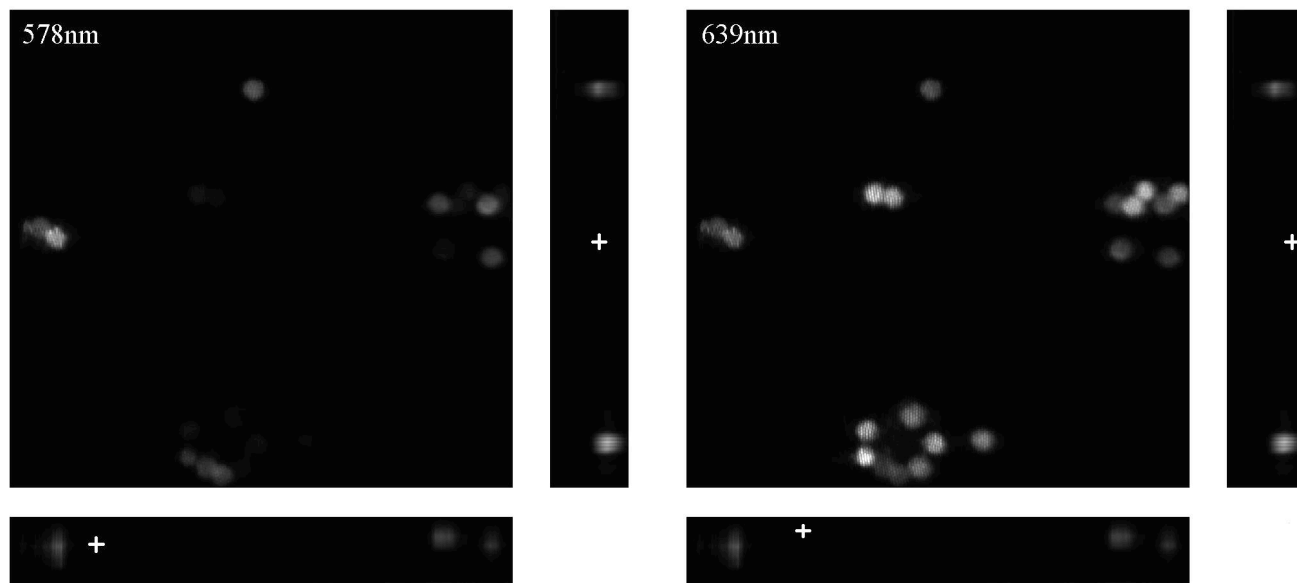

Figure 5 Fluorescence from 15μm microspheres at wavelengths of *(Left)* 578nm and *(Right)* 639nm.
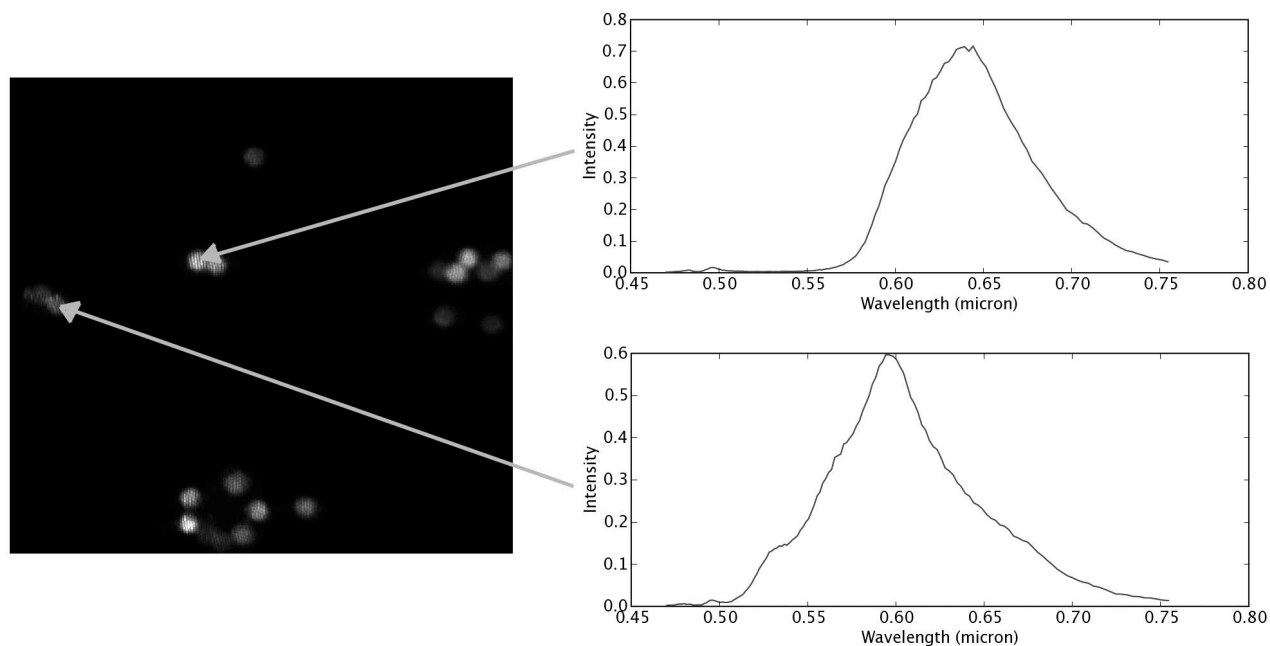

Figure 6 Fluorescence from microspheres. *(Left)* Spatial display of the unfolded multi-spectral data cube. *(Right)* Spectra at two different locations of the image.

Figures 7-10 show images of different tissue types that were stained with Acridine Orange[15] (AO). AO is a nucleic acid selective metachromatic stain that interacts with DNA and RNA through intercalation or electrostatic attraction respectively. DNA intercalated AO fluoresces green (525nm) and RNA electrostatically bound AO fluoresces red (>630nm) [16]. We used the same 488nm solid-state laser as an excitation source for these data.

Figure 7 shows images of excised human esophageal tissue stained with AO. The large structures visible in the images are characteristic of Barrett's esophagus, which is a common precursor to esophageal adenocarcinoma. The two images correspond to different wavelengths and are noticeably different. Some finer structures are visible at the high wavelength (683nm), but not at the low wavelength (540nm). We can also see from the side views, representing one spatial dimension as a function of wavelength, that there are two broad regions of fluorescence. While the fluorescence around 540nm is probably caused by the AO stained nuclei, the fine structures evident at 683nm, might be some kind of organelles, though an analysis led by a pathologist would be required in order to determine the actual nature of these structures. Figure 8 shows the spectra obtained from two different locations in the tissue sample. The spectra reveal different fluorescence peaks at the two locations. The top spectrum peaks at about 0.55μm, whereas the bottom spectrum peaks at roughly 0.68μm. This distinction confirms the previous analysis from the cross-sectional images that two different elements of the tissue are spectrally resolvable.
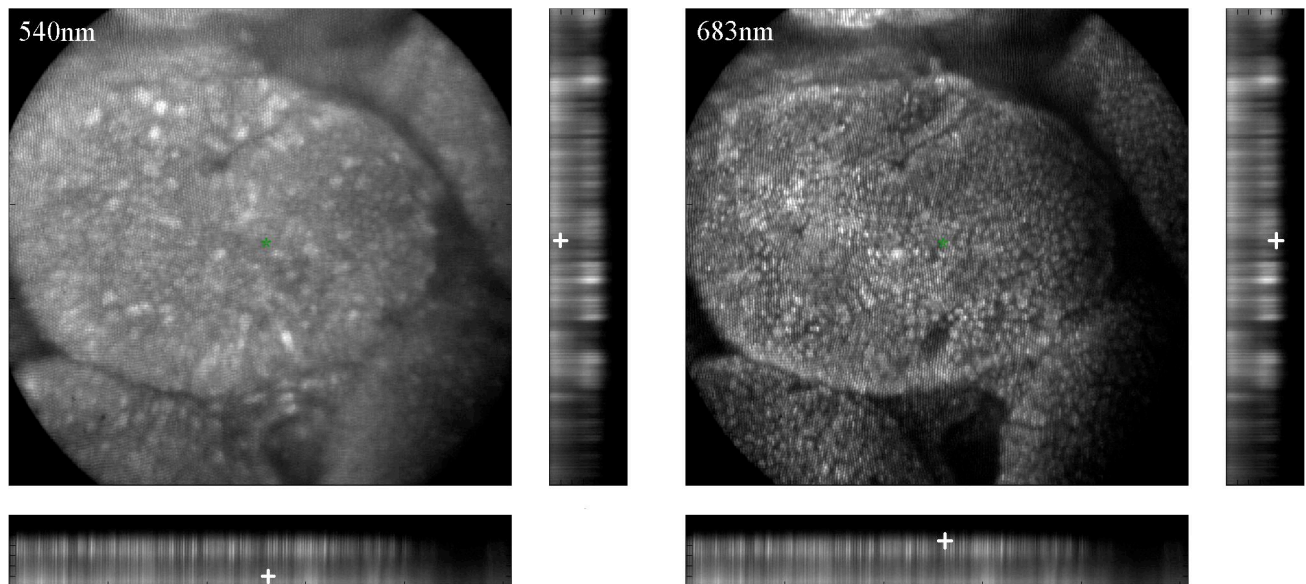

Figure 7 Excised human Barrett's esophagus tissue stained with AO and observed at wavelengths of *(Left)* 540nm and *(Right)* 683nm.
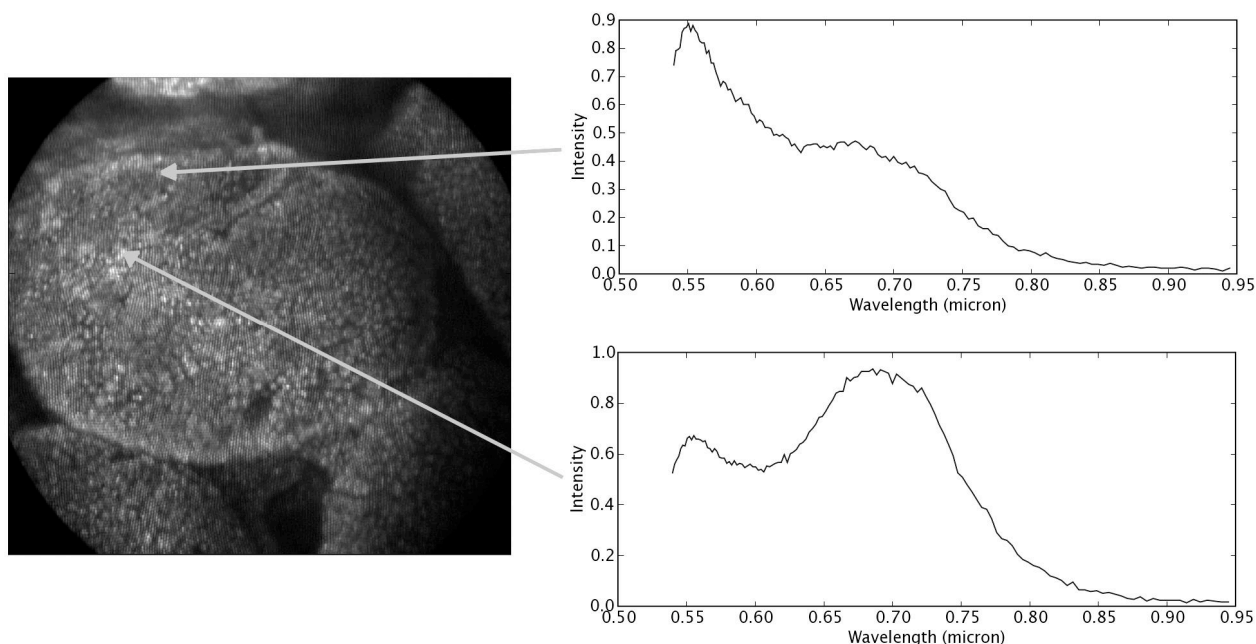
Figure 8 Excised human Barrett's esophagus stained with AO and the spectra associated with two different locations in the tissue.

Finally Figure 9 shows images of the peritoneal wall of a mouse, obtained in-situ. Again some structures, dispersed over the imaged sample, are visible at the higher wavelength (762nm), but not at the lower wavelength (572nm). These organelles might be lysosomes, which are digestive enzymes. Figure 10 represents the spectra associated with two different spots of the imaged sample; one of them corresponds to the organelles visible at higher wavelengths. The top spectrum shows a peak around 0.57μm, while the bottom spectrum, corresponding to the organelles, shows a peak around 0.74μm. Thus different elements of the tissues are distinguishable through their emission spectra.

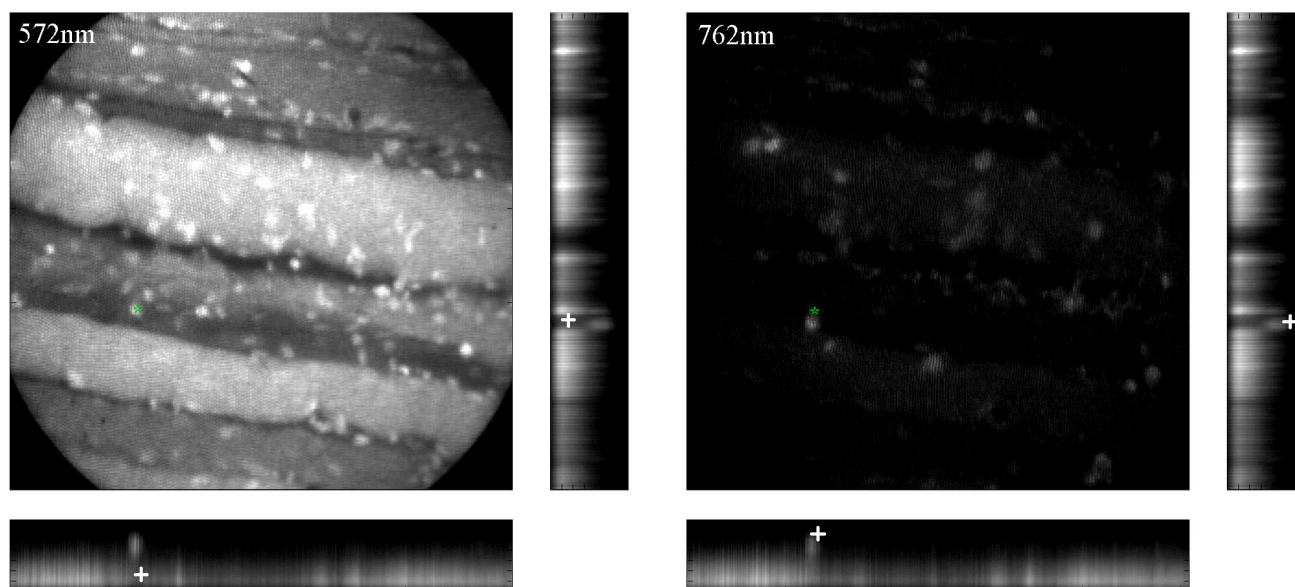**Figure 9** In-vivo images of the peritoneal wall of a mouse stained with AO at different wavelengths: *(Left)* 572nm, *(Right)* 762nm.
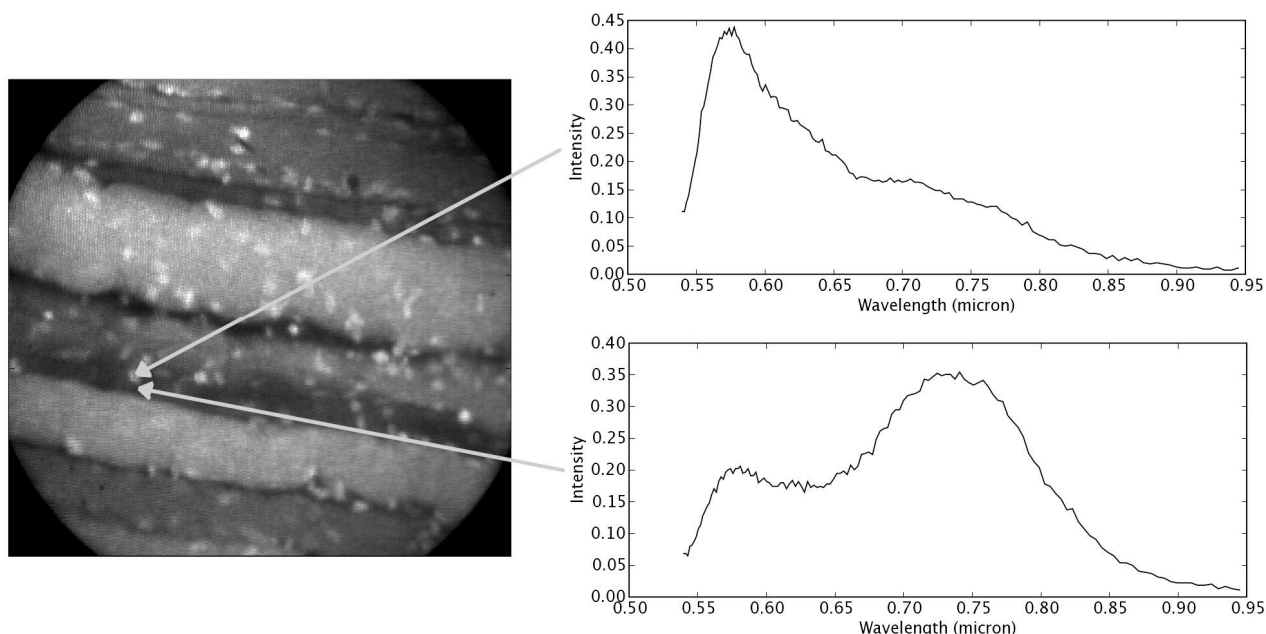
Figure 10 Mouse peritoneal wall stained with AO and the spectra associated with two different locations in the tissue.

The preceding images demonstrate that our multi-spectral confocal microendoscope can differentiate different tissue types and provide high quality images across the whole field of view. Moreover the automated system and processing software that we have developed, yields spectral information that have the potential to provide additional in-vivo diagnostic information. As a consequence, distinct elements of a given tissue sample can be highlighted when their fluorescence properties are different.

5 FUTURE WORK

Our preliminary results for the multi-spectral mode of operation are promising and we are currently investigating dyes that stain additional specific cellular contents such as mitochondria. We are also looking into the option of using a higher index glass for the prism in order to increase the spectral resolution of the system. For instance by using F2 glass instead of BK7, we could theoretically achieve a spectral resolution of 0.9nm at a wavelength of 450nm and 4.3nm at 750nm, which is roughly a two fold improvement in spectral resolution. The prism could also be replaced by a diffraction grating, which would yield a constant spectral resolution (1.2nm) with respect to the wavelength. The primary drawbacks to the grating option would be smaller transmission efficiency and a more complex geometry (additional optical components such as mirrors).

6 CONCLUSIONS

We have developed a novel confocal microendoscope system that can collect grayscale images in real time and rapidly switch to collecting spatially-resolved spectral information. We have also developed software to control the system and interactively display and explore the multi-spectral information. The gray-scale imaging mode of the confocal microendoscope has routinely provided high quality results and is currently involved in early stage in-vivo clinical trials. The multi-spectral imaging mode of the confocal microendoscope has produced excellent preliminary results. It has the same optical characteristics as the grayscale imaging mode in terms of spatial resolution, and enables the acquisition of high quality spatially localized spectra. The multi-spectral mode of our confocal microendoscope may be able to provide important diagnostic information in-vivo. By using tissue or organelle-specific fluorophores with unique spectral properties, multi-spectral imaging can separate signal from different cellular compartments and provide unique diagnostic information.

ACKNOWLEDGMENTS

REFERENCES

1. Rouse, A.R., Kano, A., Udovich, J.A., Kroto, S.M., and Gmitro, A.F., "Design and demonstration of a miniature catheter for a confocal microendoscope", Applied Optics. **43**(31) 5763-5771 (2004).
2. Rouse, A.R., Tanbakuchi, A.A., Udovich, J.A., and Gmitro, A.F., "Design of an in-vivo multi-spectral confocal microendoscope for clinical trials", in Proceedings of the SPIE The International Society for Optical Engineering: Endoscopic Microscopy. **6082** 15-22 (2006).
3. Rouse, A.R., Kano, A., and Gmitro, A.F., "Development of a fiber-optic confocal microendoscope for clinical endoscopy," in Proceedings of the SPIE The International Society for Optical Engineering: Optical Biopsy IV. **4613** 244-253 (2002).
4. Rouse, A.R., Kano, A., Kroto, S.M., and Gmitro, A.F., "Fiber optic confocal microendoscope as a daughter scope for clinical endoscopy," in Proceedings of the SPIE The International Society for Optical Engineering: Optical Fibers and Sensors for Medical Applications III. **4957** 70-78 (2003).
5. Sabharwal, Y.S., Rouse, A.R., Donaldson, L., Hopkins, M.F., and Gmitro, A.F., "Slit-scanning confocal microendoscope for high resolution in-vivo imaging", Applied Optics. **38**(34) 7133-7144 (1999).
6. Rouse, A.R., "Multi-spectral confocal microendoscope for in-vivo imaging", PhD Dissertation, Optical Sciences Center, University of Arizona (2004).
7. Rouse, A.R., and Gmitro, A.F. "Multispectral imaging with a confocal microendoscope", Optics Letters. **25**(23) 1708-1710 (2000).
8. Rouse, A.R., Udovich, J.A., and Gmitro, A.F., "In-vivo multi-spectral confocal microscopy," in Proceedings of the SPIE The International Society for Optical Engineering: Three-Dimensional and Multidimensional Microscopy: Image Acquisition and Processing XII. **5701** 73-84 (2005).
9. Srivastava, S., Rodriguez, J.J., Rouse, A.R., Brewer, M.A., and Gmitro, A.F., "Automated texture-based identification of ovarian cancer in confocal microendoscope images," in Proceedings of the SPIE The International Society for Optical Engineering: Three Dimensional and Multidimensional Microscopy. **5701** 42-52 (2005).
10. Tanbakuchi, A.A., Rouse, A.R., and Gmitro, A.F., "Surgical imaging catheter for confocal microendoscopy with advanced contrast delivery and focus systems", in Proceedings of the SPIE The International Society for Optical Engineering: Endoscopic Microscopy. **6082** 1-8 (2006).
11. Coherent (5100 Patrick Henry Dr., Santa Clara, CA 95054).
12. Oz Optics (219 Westbrook Rd, Ottawa, Ontario, K0A 1L0, Canada).
13. Sumitomo Electric USA (21221 S. Western Ave, Suite 200, Torrance, CA 90501).
14. Photometrics (3440 E. Britannia Dr., Tucson, AZ 85706).
15. Molecular Probes (29851 Willow Creek Rd, Eugene, OR 97402).
16. Website http://www.med.umich.edu/flowcytometry/.